VERTICAL REFLECTOR FIELD: FEASIBILITY OF OPTICAL AND GEOMETRICAL ARRANGEMENTS FOR CSP INTEGRATION IN FAÇADES

Aurelio González[1], Sara Cesar Chapa[2], José Gonzalez-Aguilar[1] and Manuel Romero[1]

[1] Institute IMDEA Energy, Móstoles (Spain)

[2] Leunam Gestion S.L., Boadilla del Monte (Spain)

1. Introduction

One of the short-term priorities for renewable energies in Europe is their integration for local power supply into communities and energy islands (blocks of buildings, new neighbourhoods in residential areas, shopping centers, hospitals, recreational areas, eco-parks, small rural areas or isolated ones such as islands or mountain communities) These applications strongly influence field concepts leading to modular systems capable to more closely track demand tracking, meet reliability requirements with fewer megawatts of installed power and spread construction costs over time after output has begun. In addition, integration into single-cycle high-efficiency gas turbines plus waste-heat applications clearly increments the solar share (Romero *et al*., 1999; Gonzalez *et al*., 2010).

Table 1 summarizes an overview on potential concentrating photovoltaics (CSS) integration in buildings (Chemisana, 2011). Besides, other interesting building integration solutions have been deeply analyzed, particularly those related to ready-to-use façade integration (some examples are illustrated in Fig. 1).

In this work, it is presented a feasibility study based on optical analysis of an innovative concept integrating a concentrating solar system in buildings and the main guidelines for developing it from an architectural point of view. Figure 2 shows an example of the proposed system, named Vertical Reflector Field or Vertical Heliostat Field (VHF). It is based on central receiver concentrating solar technology. A south-façade is used as reference frame for installing a heliostat field. Radiation coming for the Sun towards the south-façade is redirected by the heliostats towards a receiver placed in front of the solar field.

Tab. 1: Classification of concentrated systems applied to building integration (adapted from (Chemisana, 2011)). Notation: NTS, non-tracking systems; TAT/ESM, two-axis tracking and entire system movement; OAT/ESM, one-axis tracking and entire system movement.

	1-High Concentration C > 100x	**2-Medium Concentration (10x < C < 100x)**	**3-Low Concentration (C < 10x)**
Systems	1.1 - Point focus Fresnel systems (TAT/ESM) 1.2 - Cassegrain Optics Concentrators, (Gordon, Feuermann, 2005) (TAT/ESM) 1.3 - Light guide Solar Optics Concentrators (TAT/ESM)	2.1 - Parabolic Trough Concentrators (OAT/ESM) 2.2 - Linear Fresnel reflectors (TAT/ESM) 2.3 - Linear Fresnel lenses (TAT/ESM; OAT/ESM)	3.1 - V-Trough (NTS) 3.2 - CPC-Compound Parabolic Concentrators (NTS) 3.3 - Fluorescent Concentrators, Quantum dot Concentrators and Holographic Concentrators (NTS)
Advantage	Electrical production efficiency	(2.3) Separate the beam from the diffuse solar radiation. Interior illumination building control feasibility Optical and structural cost effectiveness	Low-cost Concentrate direct and diffuse radiation Flexible aesthetical façade
Disadvantage	Requires high precision	Overheating of Linear CPVs systems.	(3.1 and 3.2) reduce interior lighting
Integration	Flat roofs	(2.1) flat roofs, (2.2 and 2.3) flat or inclined roofs and façades.	At any building location

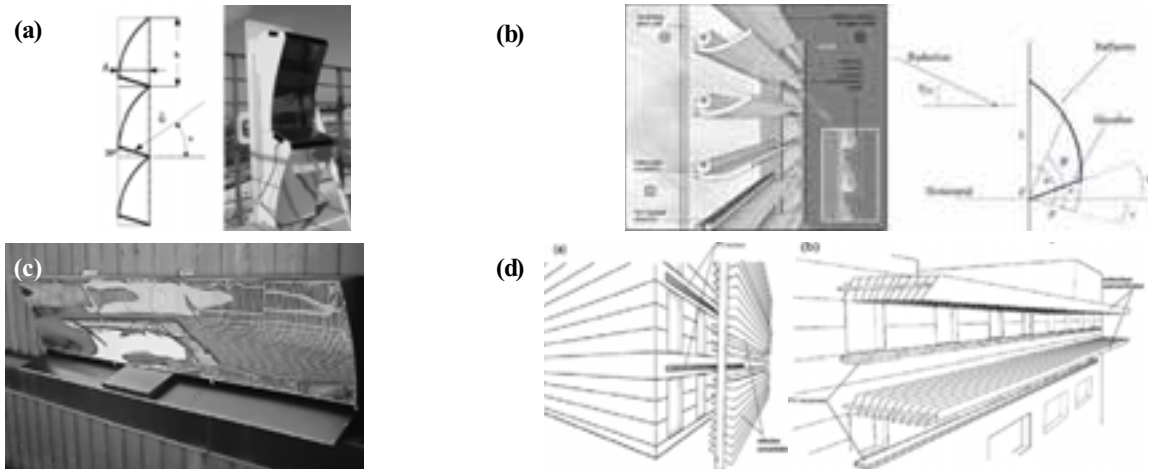

Fig. 1: (a) Concentrating PV wall element section (Brogen *et al.*, 2003); (b) Left: solar window, Right: parabolic reflector and the absorber (Davidsson *et al.*, 2010), (c) Siemens PV module reflector concentrating system (Gajbert *et al.,* 2007), (d) Left: Curtain wall architectural design, Right: Parasol architectural design (Chemisana, 2011).

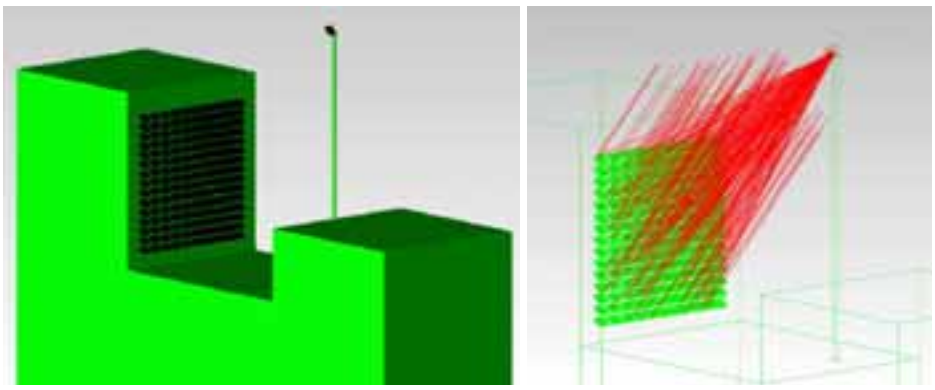

Fig. 2: (Left) Artistic view of a Vertical Reflector Field; (Right) Ray tracing of a 100kW$_{th}$ plant.

2. Optical analysis

2.1. Description of the concentrating solar system components

In order to perform the feasibility analysis, it has been defined a reference case consisting in a 100 kW$_{th}$ Vertical Heliostats Field installed in Móstoles, Spain (40º Lat.). Design point is noon time of Julian Day 81 with a nominal DNI of 850 W/m^2.

Vertical Heliostat Field (VHF). It is composed by 196 heliostats placed on the south building façade. Each heliostat has a 1-m^2 square mirror with 0.90 reflectivity and 2.6 mrad optical error (reflected ray). Among the different technologies of reflectors available today, small heliostats adapted from existing façade shading elements have been selected in order to minimize the structural stress loads.

For including the influence of the distance between heliostats edges or heliostats spacing, three distances have been taken into consideration: 1 m, 0.5 m and 0.01 m. These distances are compatible with a small occupation area, a major concern as strong constraint in urban integration.

Three different types of architectural configurations have been analyzed and evaluated under optical efficiency terms (see fig. 3): (1) Tower-type façade, corresponding to office buildings, (2) Square-type façade, related to housing buildings, and (3) Wide-type façade, associated to shopping centers or malls. Square Buildings are representative of those fields that have similar horizontal (x axis) and vertical (z axis) dimensions. Tower buildings fit into slim fields where vertical dimension is larger than the horizontal.

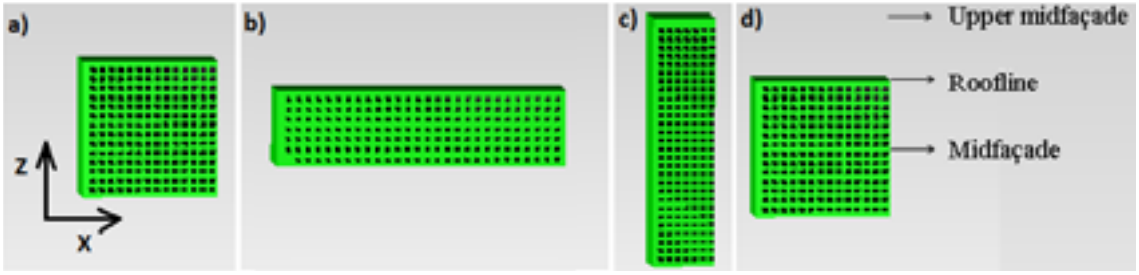

Fig. 3: (a) Square-type, (b) Wide-type, and (c) Tower-type geometries; (d) Receiver locations.

Finally, the wide-type configuration fits into fields where horizontal dimension is larger than vertical one.

Tower. Receiver position is crucial for establishing solar power plant performance. In the present work, it is assumed that receiver is placed on North-South axis at 20 m from the VHF (N-S axis crosses thru the center of the VHF). Besides, required annexed spaces for power generation, thermal storage and/or control system are supposed to be located at the same front building.

Once the tower location fixed, three different heights have been considered, corresponding to the mid façade, roofline and upper mid façade of the façade on which the VHF is installed (see Fig.1).

Receiver. It has been considered a common aperture size of 0.6 m in diameter. Although the receiver design is out of scope in the present work, its choice would depend on the power of the plant, and it could be used to solarize a gas turbine, Stirling engine, heating water, etc. A suitable non-glints receiver design proposed by Imenes and Mills (2004) is showed in figure 4. This design would avoid undesired glare effects in urban environment.

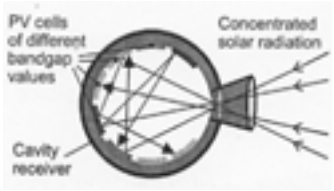

Fig. 4: Cavity receiver with PV cells as a solution for avoiding glare effects (Imenes and Mills, 2004).

2.2. Computational modelling

Calculations have been performed in three representative days: vernal equinox (day 81), summer solstice (day 172) and winter solstice (day 355). VHF receives solar radiation from 6 a.m. until 6 p.m. on day 81, sunrise and sunset, respectively. On day 172, VHF receives solar radiation approximately from 8 a.m. until 16 p.m., and further this time, even if the sun keeps a high elevation angle, its azimuth angle is larger than -90º, which means that the sun is located behind the building where the heliostats are installed and no radiation arrives to the mirrors. On day 355, VHF also receives radiation from 8 a.m. until 16 p.m., sunrise and sunset. Annual results have been obtained taking into account the hourly results of these three days (Kistler, 1986). Receiver tilt and optimal focal length have been optimized for all computer-modeling cases in order to compare the results in their best conditions.

Considering the three VHF configurations (square, wide and tower), three receiver heights, three heliostat inter-separations, and time points, at least 1000 cases have been accomplished.

During the computer-modeling process, several software tools have been employed, such as TracePro 7.04 software (Lambda Software, 2011), based on Monte Carlo ray tracing method, Microsoft Excel and Matlab®.

2.3. Calculation results

Square-type heliostat field

Hourly global optical efficiency for square-type case is shown in figure 5. Calculations indicate that the best configuration for this typology corresponds to a heliostats spacing of 1 m and a receiver placed on the roofline. Annual optical efficiencies are collected in Table 2. Roofline is the best height receiver choice for every heliostats separation, reaching 144.86 kW_{th} in the receiver on day 81 at noon. Along the year, it is observed that the lowest efficiencies always occur in summer, mainly due to the higher sun elevation angle that causes a diminution of shadowing and blocking efficiency factor. This effect would be less pronounced when heliostats spacing increases, as can be observed in figure 5. Maximum efficiency is reached at noon in all cases along days 81 and 355; however, a local minimum appears at noon of day 172 for separations of 1 and 0.5 m, due to shadows influence. This phenomenon is particularly important in case of 0.01 m separation, penalizing the efficiency along day 172 (fig. 5.c).

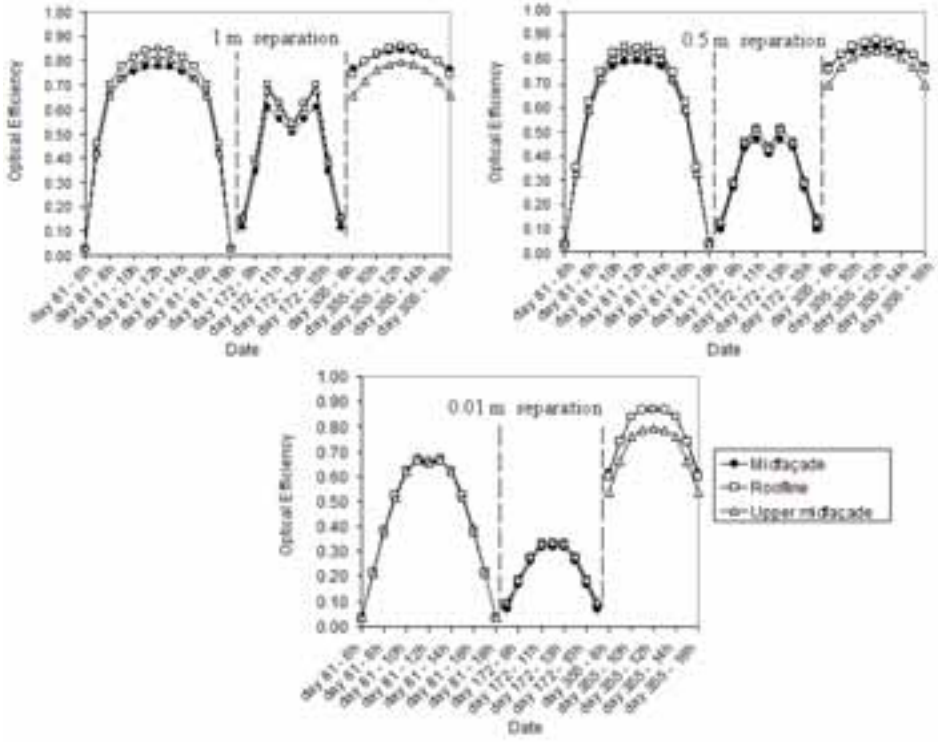

Fig. 5: Square field hourly optical efficiency values. Heliostat spacing: (a) 1 m, (b) 0.5 m, and (c) 0.01 m.

Optical efficiency factors are plotted in figure 6 in the case of receiver placed at roofline and 1 m heliostat spacing. In this case, blocking factor is almost negligible. Reflectivity factor is constant and it reduces the

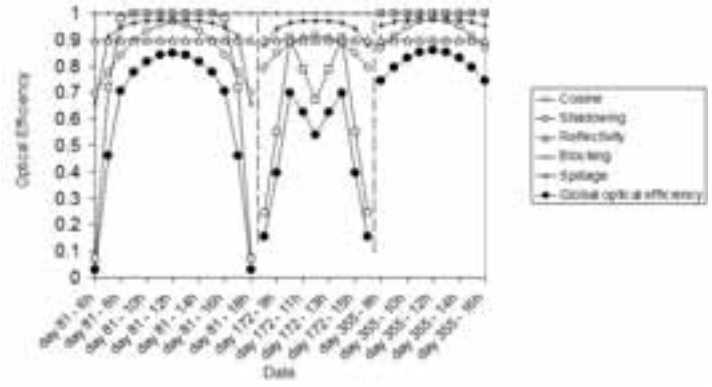

Fig. 6: Optical efficiency for receiver at roofline and 1 m heliostat spacing (Square-type heliostat field).

global optical efficiency without modifying its curve shape. Shadowing factor is almost constant achieving values close to 1 along days 81 and 355 from 8 a.m. to 4 p.m., while it shows a strong variation along 172 presenting a local minimum at noon. As it has been previously explained, this effect is related to the high sun elevation angle during the summer. Spillage factor has a similar behavior for all days, reaching maximum values at noon and slightly decreasing when it would be moving away from that time. Cosine factor also causes an important impact on global efficiency evolution. It reaches its maximum at noon. As seen in figure 6, the evolution in time of the global optical efficiency is mainly governed by blocking and cosine efficiency factors.

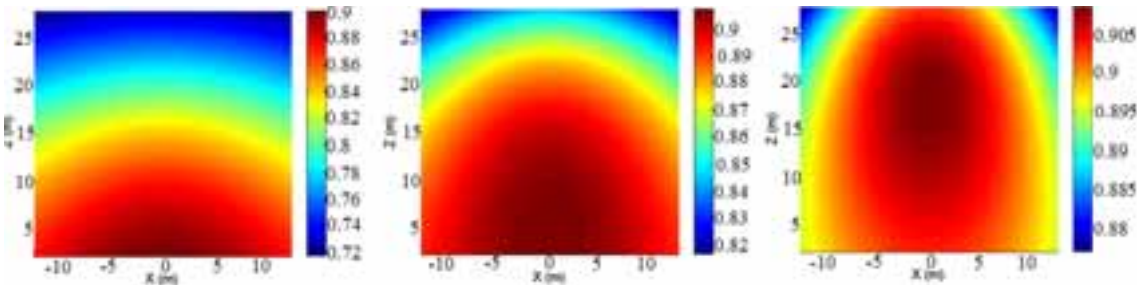

Fig. 7: Cosine factor of the square-type field for 1 m heliostat spacing and different receiver height. (Left) Mid façade, (center) Roofline, (right) Upper mid façade.

Receiver location affects drastically on optical efficiency due to its influence over cosine factor. Figure 7 depicts the annual cosine factor for each receiver position case. Distribution maximum moves upwards when receiver height increases. This trend becomes evident in the extreme case where receiver is situated in the upper mid façade. Then most active heliostats are located in the middle and upper part of the field. Annual average cosine factor for mid façade, roofline and upper mid façade are 0.82, 0.88 and 0.90, respectively.

Tower-type heliostat field

Hourly optical efficiency values are shown in figure 8. With this typology, receiver placed at mid façade is the most adequate choice, being more evident for winter season. The best configuration has a heliostat spacing of 0.5 m, achieving 124.96 kW_{th} in the design point.

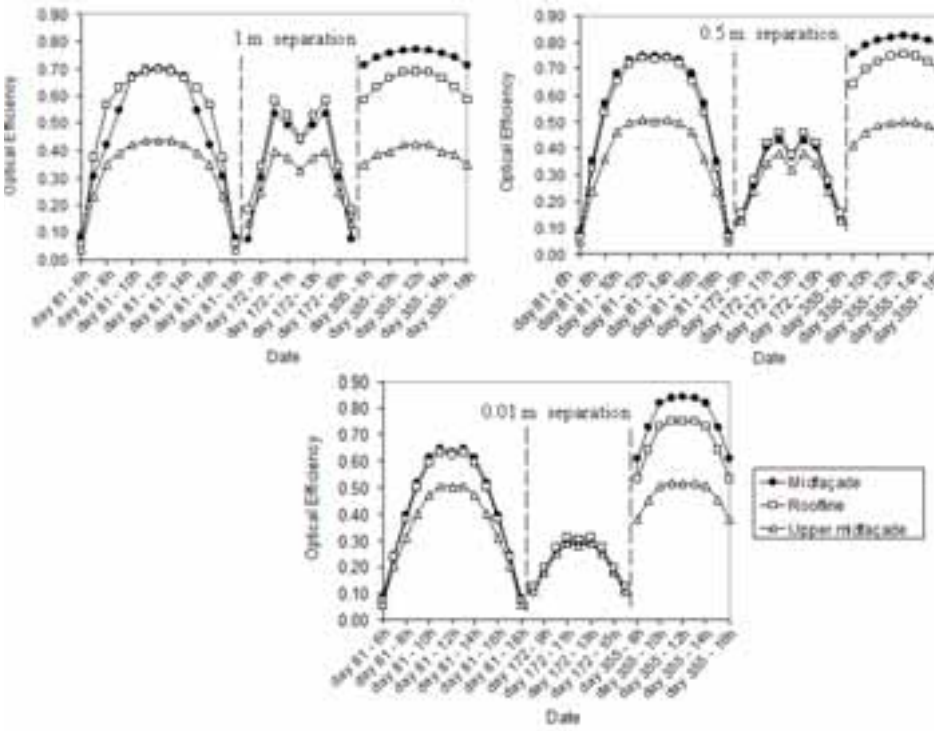

Fig. 8: Tower-type heliostat typology field hourly optical efficiency values. Heliostat spacing: (a) 1 m, (b) 0.5 m, and (c) 0.01 m.

1 m heliostat spacing case does not appear as the best option because the increment of separation between heliostats enlarges the field raising up heliostat-receiver distances and increasing spillage losses. This important influence of spillage on optical efficiency has been proved by performing calculations without taking into account spillage. In these simulations, it has been observed that best results would be obtained for 1 m separation case.

As in square-type typology, lowest efficiencies are always achieved during the summer by the same reasons descried previously. However, this effect is less pronounced when heliostats separation increases. Optical efficiency decreases drastically for upper mid façade case what reject this location for placing the receiver. In the same way, maximum optical efficiency along days 81 and 355 is achieved at noon, while it suffers a drop at midday of 172 for 1 and 0.5 m heliostat spacing by shadows effects.

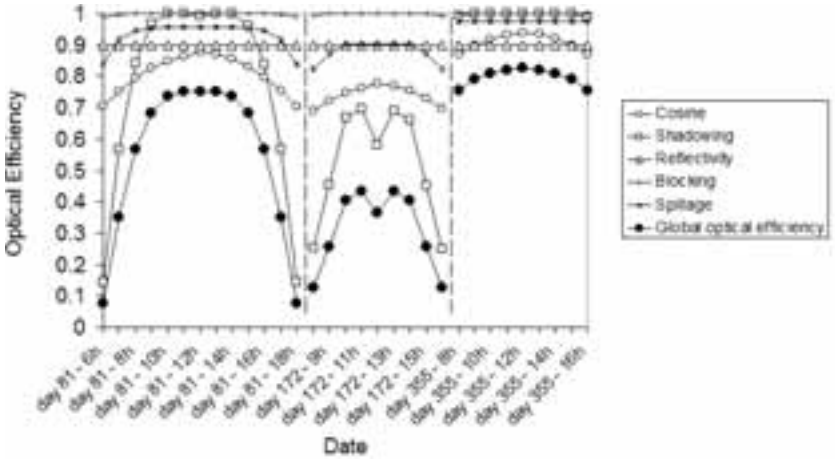

Fig. 9: Optical efficiency for mid façade receiver height / 0.5 m Heliostats edges separation for tower typology.

Optical efficiency factors have been plotted for mid façade and 0.5 m separation case in figure 9. Sun blocking is insignificant and reflectivity is a constant value that does not affect optical efficiency curve shape. Shadowing evolution shows the same behavior as in the square case, sharply dropping at noon of day 172 due to the high elevation angle of the sun. In comparison with square results, cosine efficiencies evolve in the same way along the days, but tower field has worse global optical efficiency, especially on summer time.

Figure 10 presents the evolution of the annual cosine efficiencies of the whole field, results for 0.5 m of separation and the three receiver locations. Heliostats with the best annual cosine for mid façade case are located in the lower part of the field.

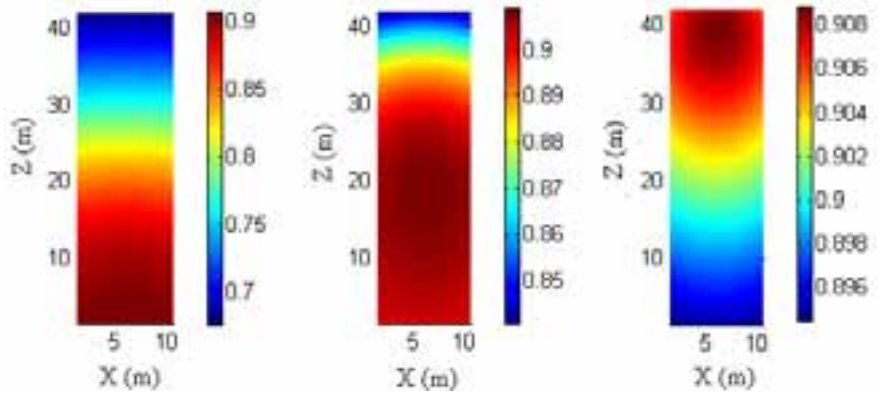

Fig. 10: Cosine factor of the tower-type field for 0.5 m heliostat spacing and different receiver height. (Left) Mid façade, (center) Roofline, (right) Upper mid façade.

Tower typology follows the same trend as square one, and the field area where heliostats have the best annual cosine efficiency moves upwards when receiver height increases. Annual average cosine factor efficiency for mid façade, roofline and upper mid façade are 0.82, 0.895 and 0.90, respectively. The low cosine factor for mid façade is offset by high shadowing efficiencies, which finally make mid façade case reachs the best annual optical efficiencies (Table 2).

Wide-type

Main results are plotted in figures 11 and 12. Calculations show that the effect of receiver height slightly affects optical efficiencies. It has to be considered that vertical dimension of the field is quite small compared with previous cases, and then differences between considered receiver locations are smaller, what minimizes efficiency variations. Best results are always obtained for receiver located at upper mid façade, and for 1 m separation case it is obtained the highest optical efficiency for that typology (tab. 2), obtaining 120.4 kW_{th} on day 81 at noon. As the best values have been obtained for the highest simulated receiver heights, it will be necessary further simulations taking into account higher heights, in order to delimit the optimum receiver position.

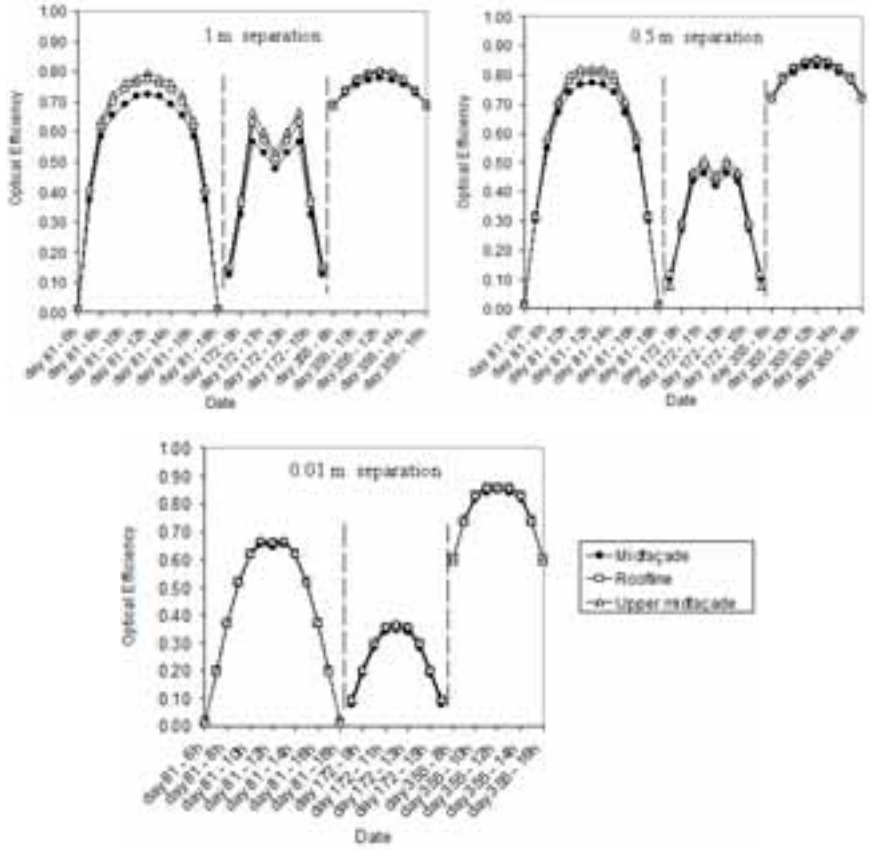

Fig. 11: Hourly optical efficiency values for "wide" typology field. a) Separation of 1 m between heliostats. b) Separation of 0.5 m. c) Separation of 0.01 m (continues down)

Factors contributing to the total optical efficiency for 1 m heliostat spacing separation and mid façade case are plotted in figure 12. Efficiencies trends are quite similar to those described in previous typologies. Shadowing is almost negligible during spring and winter, while its effect is detrimental to global efficiency in summer. Spillage and cosine are responsible for the characteristic optical efficiency curve. Annual cosine values of the heliostats field for the three studied receiver locations heliostats field are shown on figure 13.

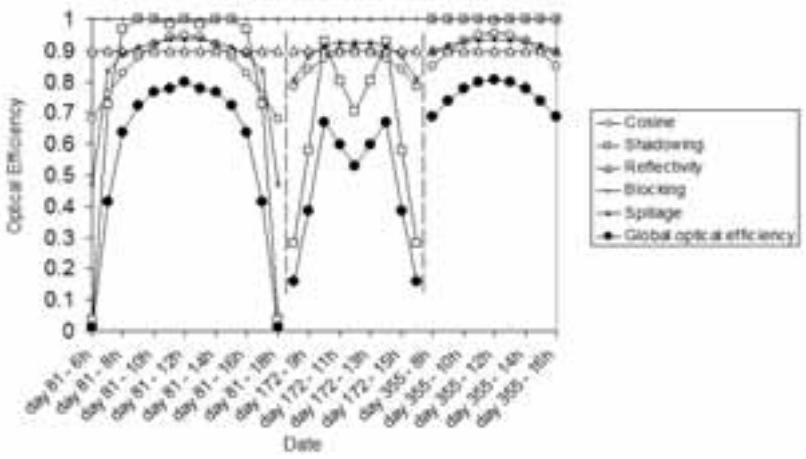

Fig. 12: Optical efficiency for midfaçade receiver height / 1 m Heliostats edges separation for wide-typology

Heliostats placed close to the façade edges present the worst results, and as previously, best efficiency area moves upwards when receiver height increases. Annual average cosine values for mid façade, roofline and upper mid façade are 0.806, 0.842 and 0.866, respectively. Compared to the other typologies, this field gets the lowest cosine efficiencies. However, it gets better annual efficiencies than the tower one.

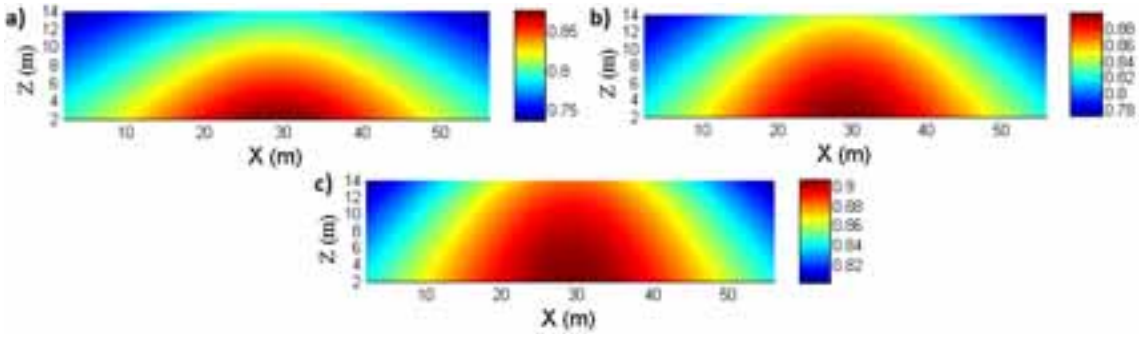

Fig. 13: Cosine efficiencies of the wide-type field for different receiver heights and 1 m heliostats separation. Left: Midfaçade. Center: Roofline. Right: Upper mid façade.

Optical efficiencies for the whole amount of studied cases are summarized on table 2. Façade occupation factor is an aspect that must be taken into account for future profitability studies. In table 3, it has been summarized the efficiency values comparing power arriving to the receiver aperture divided by the total power arriving to the whole area, it means land occupied by the field.

Façade occupation factor is an aspect that must be taken into account for future profitability studies. In table 3 it has been summarized the efficiency values comparing power arriving to the receiver aperture divided by the total power arriving to the whole area; it means land occupied by the field.

Tab. 2: Annual optical efficiency values for the whole possible simulated alternatives.

	Separation of 1 m			Separation of 0.5 m			Separation of 0.01 m		
	Mid façade	Roofline	Upper mid façade	Mid façade	Roofline	Upper mid façade	Mid façade	Roofline	Upper mid façade
Square	0.599	**0.635**	0.596	0.570	**0.596**	0.572	0.466	**0.473**	0.449
Tower	0.520	**0.524**	0.333	**0.550**	0.523	0.369	**0.465**	0.440	0.340
Wide	0.548	0.577	**0.593**	0.546	0.566	**0.573**	0.462	0.470	**0.474**

Tab. 3: Optical efficiency values in terms of total area land occupied by the field.

	Separation of 1 m			Separation of 0.5 m			Separation of 0.01 m		
	Mid façade	Roofline	Upper mid façade	Mid façade	Roofline	Upper mid façade	Mid façade	Roofline	Upper mid façade
Square	0.161	**0.171**	0.160	0.266	**0.287**	0.267	0.390	**0.396**	0.376
Tower	0.143	**0.144**	0.091	0.261	**0.247**	0.174	**0.391**	0.369	0.286
Wide	0.150	0.158	**0.163**	**0.270**	0.267	**0.270**	0.388	0.395	**0.398**

Results are better when separation between heliostats is lower. Previous efficiency analysis indicates that a separation of 0.01 m is a good choice, however further analysis including economic should be taken into account for confirming this observation.

3. Architectural Design

Figures 14 and 15 illustrate two proposals for an external steel frame structure used for supporting the heliostat field. It is built from steel columns and beams (HEB) and it allows its free structural movement from the main building envelope. This skeleton would avoid the transmission of structural overstresses to the main building owing to the continuous heliostats sun tracking movement.

The second aesthetic skin is fixed to the main façade by means of vibration isolation bearings placed between beam headings and slaps and under each heliostat foundation.

The overall movement is minimized facilitating incorporation into buildings and offering different possibilities for the façade composition.

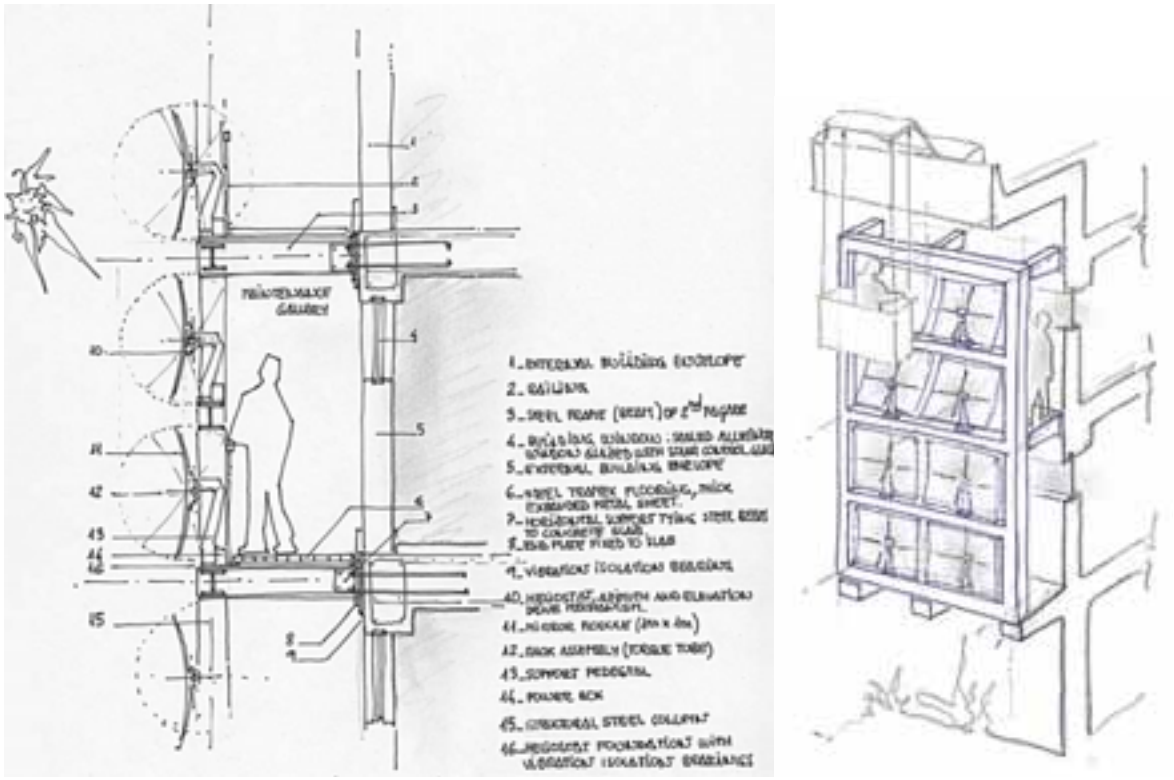

Fig. 14: 1st concept of CSP system integration in building. (Left) Typical cross façade section; (right) Steel frame structure.

There is an outdoor maintenance walkway between the heliostat façade and the external enclosure of the building, making easier any Maintenance & Operation task. Notice that the sketches just represent the architectonical concept, without measurement or scale, so loadings, structural stresses and reactions must be considered to select the appropriate standard steel member of which section and properties satisfy the mechanical design requirements. In addition, the annexed areas requirements must be considered, including tower needs and receiver features (materials, dimensions and non-glint design).

A more innovated solution, formulated from the building roof as the Fifth Façade, is illustrated in figure 15. The heliostat field support mimics an armadillo carapace and so taking advantage of the entire envelope (exo skeleton) of the building, when architecture design makes it possible. This proposal would be associated to a multi-tower system (Fig 15).

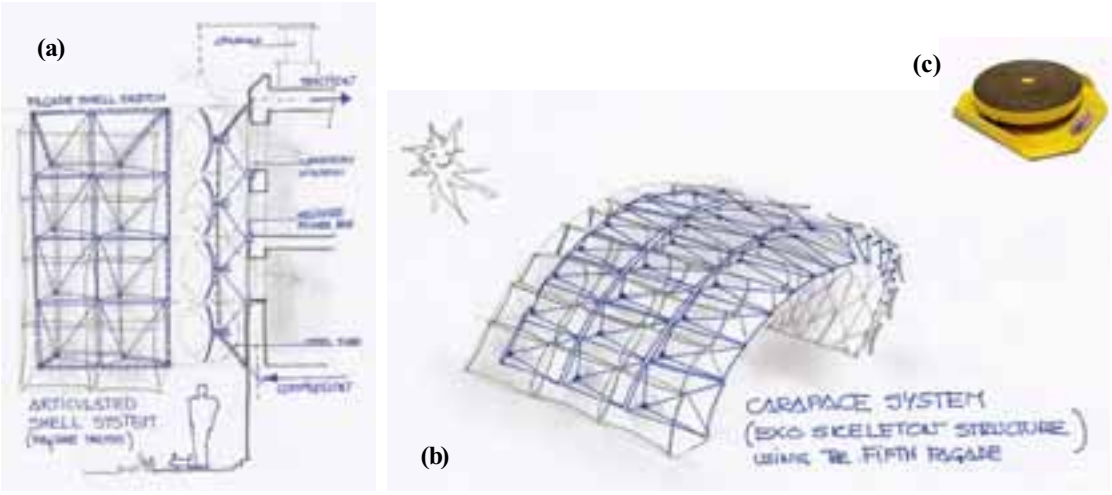

Fig. 15: 2nd concept of CSP system integration in building (a) Façade and cross section of the articulated shell heliostat system; (b) 3D articulated shell heliostat system; (c) Individual Heliostat Vibration isolation bearing photo.

4. SWOT Analysis of the CSP building integration

Tab. 4: Analyses of competitive advantages of CSP building integration systems.

STRENGHTS	WEAKNESSES
Electricity production efficiency Dispatchable energy (Energy-Heat Storage can be solved by using molten salt and others) Thermal storage improves capacity factor Proven and mature technology Fuel supply is free and renewable The entire systemuses established technology that is ready available (mirrors, tubes and electrical generators). CSP can store the collected energy as heat, cheaply and easily in many designs The heat can be used to generate steam/electricity on demand, cooling, air-conditioning, desalination, co-generation, etc. Environmentally friendly	Mirrors prevent light from passing into the building The heliostat movement creates strain on the building structure. O&M costs may also be higher for concentrating systems due to the tracking actuators. Cost of electricity generated from CSP, at urban scale, is higher than conventional technologies. Excellent solar conditions (direct irradiance) are required. Tower receiver environmental glare. Planning regulations (tower height, and aesthetical façade regulations). Central receiver has not been demonstrated at commercial scale in urban communities.

OPPORTUNITIES	THREATS
Urban planning application based on District heating production, bulk gridding integration for cities, dispatching heat, electricity and others on demand. Innovated architectonical building integration, generating functional façades from technology beauty.	Building integration competitors: CPV technology Planning Regulations Population has no knowledge about this technology as an efficiency energy resource applied to buildings energy demands

5. Conclusions

A new concept integrating a concentrating solar system in buildings, called Vertical Reflector Field or Vertical Heliostat Field (VHF), has been described. The optical analysis of several VHF configurations makes possible a better understanding of the performances of this kind of facilities. The comparison between square, tower and wide-type configurations suggests that square-type provides better optical efficiencies than the others.

Optical efficiencies breakdowns show that similar trends are followed by the three configurations. Sun blocking effect is negligible along the whole year for all the cases, while shadowing plays an important role in the behavior of the field: worst results are obtained always for summer time, mainly due to the high elevation angle of the Sun that produces higher shadowing losses. During this season there are less working hours due to azimuth angle reaches values further than 90º, and this effect is not specific for VHF but common for every solar energy system integrated into façades.

Cosine factor also plays an important task in optical efficiency evolution and field area that contains heliostats with better cosine efficiencies moves upwards when receiver height increases. In terms of receiver heights, roofline tower height is the best option for square typology, while tower field works better in mid façade height option in almost cases, and wide-type field would do its best when upper mid façade heights and even further were running.

Further analyses are going to be carried out in order to study in depth the annual efficiencies of different heliostat field zones. In this paper, a regular grid has been used for heliostats arrangements, but further studies would be performed in order to test different layouts as radial traditional one (Kistler, 1986), in the way of searching the best options. Besides, it would be important to deeply analyze the influence of others heliostats parameters such as the height to width heliostat ratio or use of several focal distances. Finally, Global efficiency of the whole facility, including receiver design options and performances as well as power block, would lead us to an accurate knowledge of the overall system efficiency.

Annual optical efficiencies for the best cases reach values that are closed to traditional horizontal field arrangements, what supports the feasibility of Vertical Heliostats Field.

6. Forward Vision

CSP integration in buildings is feasible, both in technical and optical efficiency terms. It is just a question of time. Environmental awareness and maybe evolution will do the rest…

Fig. 16: (Left) 2010, Solar power offices in Ljubljana, Slovenia, by OFIS Architects. CO_2 neutral building, (Center) 1997-2004, The Sage Gates head, UK, by Foster + Partners, (Right) 2011..., Armadillo and its carapace.

7. Acknowledgements

The authors wish to thank “Comunidad de Madrid” and “European Social Fund” for its financial support to the SOLGEMAC Project through the Program of Activities between Research Groups (S2009 ENE-1617).

8. References

Brogren, M., Wennerberg, J., Kapper, R., Karlsson, B., 2003. Design of concentrating elements woth CIS thin-film solar cells for façade integration. Solar Energy Materials & Solar Cells 75, 567-575

Chemisana, D. 2011. Building integrated concentrating photovoltaics: a review. Renewable and Sustainable Energy Reviews, 15, 603-611

Davidsson, H., Perers, B., Karlsson, B., 2010. Performance of a multifunctional PV/T hybrid solar window. Solar Energy 84, 365-372.

Gajbert, H., Hall, M., Karlsson, B., 2007. Optimisation of reflector and module geometries for stationary, low-concentrating, façade-integrated photovoltaic systems. Solar Materials & Solar Cells 91, 1788-1799.

González A., González-Aguilar J., Romero M., 2010. “Integration of a solar tower field in a car parking lot: a new concept of distributed power generation”. SolarPACES 2010. 21-24 September 2010, Perpignan, France.

Kistler, B., 1986. A User’s Manual for DELSOL3: A Computer Code for Calculating the Optical Performance and Optimal System Design for solar Thermal Central Receiver Plants. SAND86-8018

Imenes, A., Mills, D., 2004. Spectral beam splitting technology for increased conversion efficiency in solar concentrating systems: a review. Solar Materials & Solar Cells 84, 19-69.

Lambda Software, TracePro v7.4 2011. Available from: <www.lambdares.com>.

Romero, M., Marcos, M.J., Téllez, F., Blanco, M., Fernández, V., Baonza, F., Berger, S., 1999. Distributed power from solar tower systems: A MIUS approach. Solar Energy, 67, 249-264.